Proceedings of the International MultiConference of Engineers and Computer Scientists 2009 Vol II
IMECS 2009, March 18 - 20, 2009, Hong Kong

Numerical Simulation of Sintered Perforated Hollow Sphere Structures (PHSS) to Investigate Thermal Conductivity

Andreas Öchsner *, Seyed Mohammad Hossein Hosseini †, Markus Merkel ‡

Abstract—**This paper investigates the thermal properties of a new type of hollow sphere structures. For this new type, the sphere shell is perforated by several holes in order to open the inner sphere volume and surface. The effective thermal conductivity of perforated sphere structures in several kinds of arrangements is numerically evaluated for different hole diameters. The results are compared to classical configurations without perforation. In the scope of this study, three-dimensional finite element analysis is used in order to investigate simple cubic, body-centered cubic, face-centered cubic and hexagonal unit cell models. A linear behavior was found for the heat conductivity of different hole diameters for several kinds of arrangements when the results are plotted over the average density.**

Keywords: ***Cellular materials, Thermal conductivity, Finite element method.***

1 Introduction

Hollow sphere structures (HSS) are novel lightweight materials within the group of cellular metals (such as metal foams) which are characterised by high specific stiffness, the ability to absorb high amounts of energy at a relatively low stress levels, potential for noise control, vibration damping and thermal insulation, cf. Fig. 1. A combination of these different properties opens a wide field of potential multifunctional applications e.g. in automotive or aerospace industry. Typical functional applications of cellular metals in the scope of heat transfer are heat exchangers [1, 2, 3], fire retardance systems [4] or thermal insulation. The high thermal insulation capability of hollow sphere structure has been addressed in a US Patent [5] by Schneider and co-workers. Baumeister and colleagues [6] investigated the linear thermal expansion coefficient of corundum based hollow sphere composites (HSC) using thermomechanical analysis. They found that the thermal behaviour of HSC is mainly governed by the epoxy resin. Lu and Kou [7] conducted a comprehensive numerical and experimental study based on unit cells of homogeneous hollow sphere structures. However, only automatically generated finite element meshes were used and the applied approach does not allow the consideration of different material combinations. In recent paper [8], the thermal conductivity of adhesively bonded and sintered HSS was numerically investigated while in paper [9], the influence of material parameters and geometrical properties of syntactic (hollow spheres completely embedded in a matrix) and partially bonded HSS (spheres joined in localised contact points) was analysed. A comparison between analytical, numerical and experimental approaches is given in [10]. Fiedler et al. reported in [11] recent advances in the prediction of the thermal properties of syntactic metallic hollow sphere structures. They described the application of the Finite Element and Lattice Monte Carlo Method in the case of syntactic periodic and random hollow sphere structures. Manufacturing techniques for perforated hollow sphere structures are actually under development [12] and we use an idealised model structure to clarify basic effects of the perforation on physical properties.

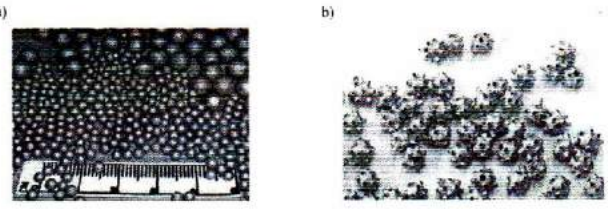

Figure 1: Single hollow spheres: a) closed surface (common configuration); b) with perforated surface (new development); (©by Glatt GmbH, Dresden, Germany).

In the present study, perforated hollow spheres arranged in several types of periodic pattern are numerically investigated based on the finite element method (unit cell approach) and the effective thermal conductivity is com-

*Department of Applied Mechanics, Technical University of Malaysia, 81310 Skudai, Malaysia & Centre for Mass and Thermal Transport in Engineering Materials, The University of Newcastle, Callaghan, New South Wales 2308, Australia, Email: Andreas.Oechsner@gmail.com

† Department of Applied Mechanics, Technical University of Malaysia, 81310 Skudai, Malaysia, Email: rsg.931@gmail.com

‡Department of Mechanical Engineering, University of Applied Sciences Aalen, 73430 Aalen, Germany, Email: Markus.Merkel@htw-aalen.de

pared to structures without holes. The influence of the hole diameter and the geometry on the effective conductivity is analysed within a parametric computational study.

2 Mnufacturing

A powder metallurgy based manufacturing process enables the production of metallic hollow spheres of defined geometry [13]. This technology brings a significant reduction in costs in comparison to earlier applied galvanic methods and all materials suitable for sintering can be applied. EPS (expanded polystyrol) spheres are coated with a metal powder-binder suspension by turbulence coating. The green spheres produced can either be sintered separately to manufacture single hollow spheres or be precompacted and sintered in bulk (cf. Fig. 2) thus creatingsintering necks between adjacent spheres [14].

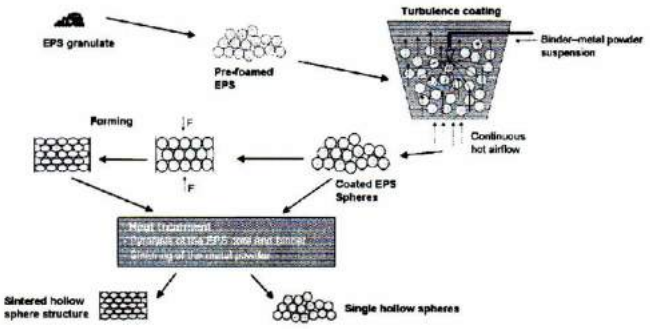

Figure 2: Manufacturing processes of single hollow spheres and hollow sphere structures [12].

Depending on the parameters of the sintering process the micro-porosity of the sintered cell wall can be adjusted. In a subsequent debindering process, the EPS spheres are pyrolised. The increase of the carbon content of the sintered metal by the diffusion of the incinerated binder and polymer causes degradation of mechanical properties and corrosion resistance. Special reducing processes are required to reduce this effect [15]. Various joining technologies such as sintering, soldering and adhering can be used to assemble the single hollow spheres to interdependent structures [16, 17].

3 Perforated Hollow Sphere Structure

The major idea of introducing a perforation, i.e. holes of circular cross section in the sphere shells, is to make the inner sphere surface and volume usable. In this paper, the holes are defined in such a way that the largest possible hole can be located between the sintering areas in a primitive cubic arrangement. In subsequent steps, the size of this initial hole was gradually reduced in the other models with different types of arrangements. Our modeling approach is restricted to the simple case where the holes do not intersect with the sintering area. The additional inner surface may be used for chemical reactions in the case of catalysts or the additional inner volume may have a positive influence on the dissipation of e.g. acoustic waves. A simplified arrangement of perforated hollow sphere structures in a primitive cubic pattern is shown in Fig. 3.

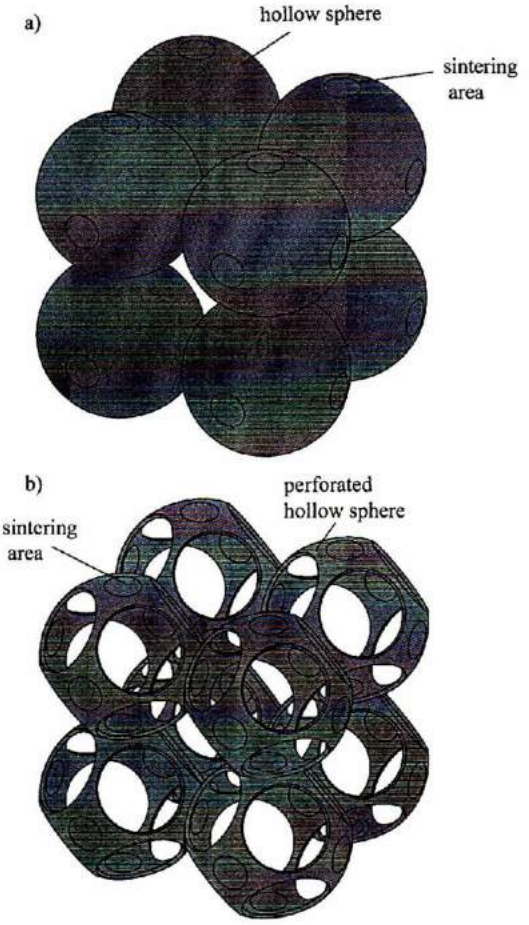

Figure 3: Schematic representation of primitive cubic sphere arrangements: a) sintered classical hollow sphere structure; b) sintered perforated hollow spheres structure.

Looking at a specific example where perforated spheres (outer diameter 2.7 mm and shell thickness of 0.1 mm, outer hole radius 0.68 mm) are considered, the available free surface increases by ~57% and the free volume increase by ~259% while the bulk volume or the weight is reduced by ~33%. In addition, we can state that the porosity is only increased by ~3.9%.

3.1 Modeling of Perforated Hollow Sphere Structures

Since the aim of this research is to highlight the difference between perforated and entire spheres (cf. Fig. 3) to investigate the influence of perforation on the heat con-

ductivity, different CAD models were used. By means of an image processing software, a series of micrographs was analysed and geometrical values for different model structures are derived [18], cf. Fig. 4,8 and Tab. 1.

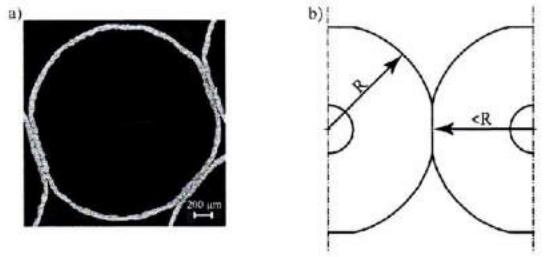

Figure 4: a) Photo of a sintered hollow sphere structure; b) Schematic sketch of a sintered hollow sphere structure.

In order to reduce the size of the system of equations, the so-called unit-cell approach is chosen where the computational structure is reduced from a larger or infinite amount of randomly arranged spheres to a single unit-cell which is commonly based on typical space groups as in crystallography [19]. This is a first estimation for a finite element analysis that can give reasonable results. Common unit cell approaches are based on primitive cubic, face-centered, body-centered or hexagonal arrangements, cf. Fig. 5.

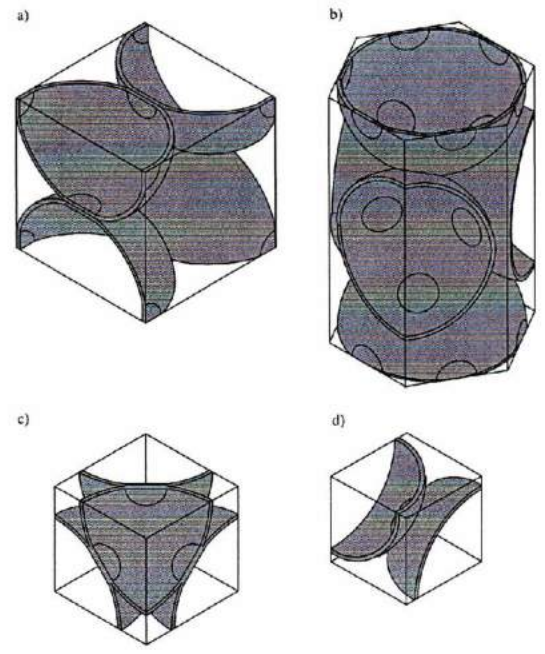

Figure 5: Unit cell models for sintered spheres: a) primitive cubic (entire UC); b) hexagonal (entire UC); c) face-centered cubic (one-eight of UC); d) body-centered (one-eight of UC).

4 Finite Element Approach: Geometry and Mesh

Finite element analysis demands the discretisation of the geometries by subdividing them into geometrically simple finite elements. In the scope of these analyses, primarily three-dimensional geometries are considered. For the three dimensional meshing, tetrahedral or hexahedral elements can be employed. Earlier investigations [20, 21] have shown that hexahedral elements yield superior performance. Therefore, the geometry of the structures is discretised based on regular hexahedral elements. This approach is much more time-consuming, but it is important in order to achieve more accurate simulations. The meshing of the micro-structure of MHSS requires the decomposition of these complex geometries into simple subgeometries. Based on the obtained fragments, meshing algorithms can be applied in order to obtain regular hexahedral meshes [22]. Therefore, these sub-geometries have to exhibit a principally cubical shape. Figure 6 demonstrates the decomposition of a syntactic face centered cubic geometry.

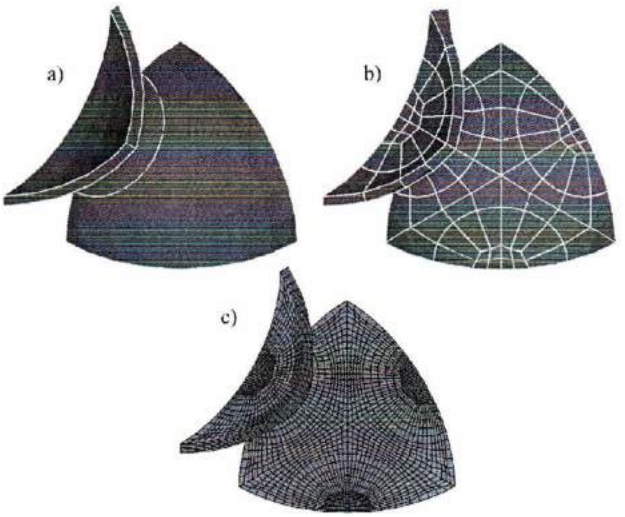

Figure 6: Generation of the computational FCC model (one-twenty four of UC): a) CAD geometry; b) subdivision of the solid geometry in simple parts; c) entire mesh.

In order to minimise the number of fragments, symmetries are exploited. In the example shown, only $\frac{1}{24}$ of the final model sub-geometries need to be meshed and, by mirroring rest of fragments are obtained which assemble to the target geometry (cf. Fig. 7).

5 Finite Element Method and Basics of Heat Transfer

A typical finite element mesh including boundary conditions is shown in Fig. 8. Constant temperature boundary conditions ($T_i = const.$) are prescribed at the faces

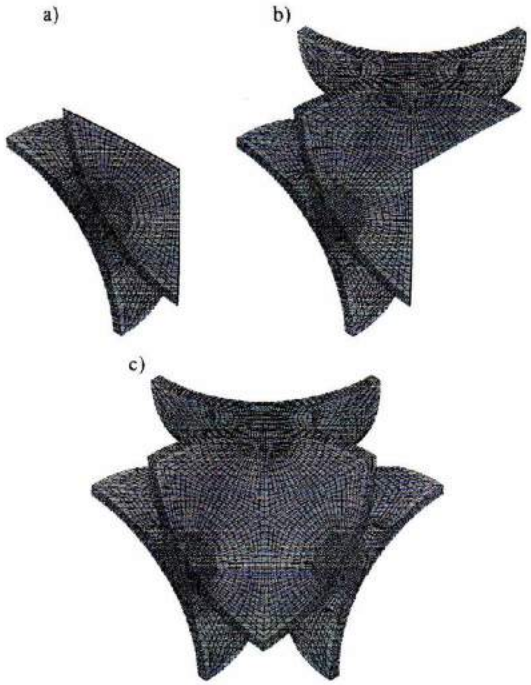

Figure 7: Generation of the computational FCC model: a) one-twenty four of UC; b) one-twelve of UC; c) one-eight of UC.

of the connective elements on the left and right side of the model. In order to generate a heat flux through the structure, only $T_1 \neq T_2$ must be fulfilled.

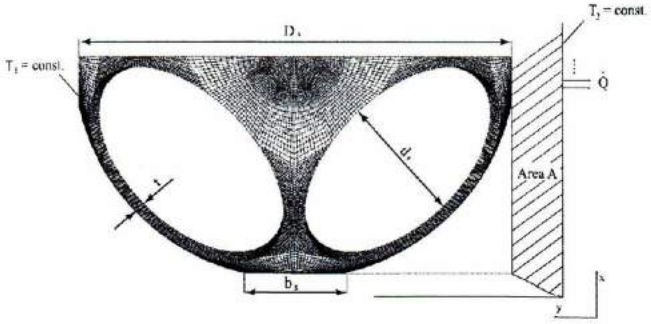

Figure 8: Finite element mesh and boundary conditions of a sintered perforated primitive cubic unit cell.

According to the assumed symmetry and simplifications (no radiative or convective effects), the ratio of the heat flux perpendicular to all remaining surfaces is zero. The thermal properties of the considered base material is for steel $k_{\text{steel}} = 0.05$ W/mm·K (AISI 8000).

The evaluation of the effective thermal conductivities within the finite element approach is based on Fourier's law where the area-related conductivity is defined by

Dimension	Value [mm]
D_s	2.66
b_s	0.6
d_s	1.47
t	0.1

Table 1: Sphere dimensions.

$$k = \frac{\dot{Q}}{A} \cdot \frac{\Delta y}{\Delta T} \tag{1}$$

The area A of the unit cell and the spatial distance Δy are given by the geometry (cf. Fig. 8), respectively the temperature gradient $\Delta T = T_2 - T_1$ by the boundary conditions, only the heat flux $\dot{Q}$ remains to be determined. This is done by summing up all nodal values of the reaction heat flux with a user subroutine at the left or right face where a temperature boundary condition is prescribed. Within the relevant temperature range, the contribution of thermal radiation to the heat transfer is low [4]. Furthermore, contributions from gaseous conduction and convection are neglected. The whole model consists of 51056 elements in the case of the largest hole with a radius of 0.68 mm. Subsequent models where the hole diameter was reduced to 75, 50 and 25% where generated. Figure 9 summarises the influence of mesh density on outcomes results for heat conductivity, calculated by the finite element code. One can observe that increasing the mesh density results in a stable value of conductivity. Thus, as indicated in the figure, a choice of 27292 elements is reasonable to calculate the heat conductivity.

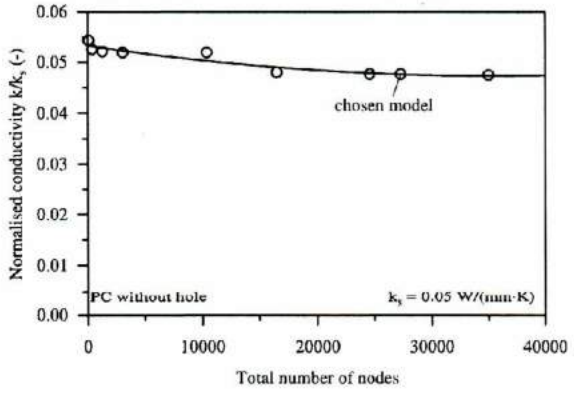

Figure 9: Results of mesh refinement analysis.

All the simulations were done with the commercial finite element package MSC.Marc ©(MSC Software Corporation, Santa Ana, CA, USA).

6 Average Values for Cellular Metals

The average density (Eq. 2) is an common value to make a statement on the density, mass, weight and further

lightweight parameters. Physical properties are commonly described as a function of their average density [23]

$$\varrho_{\text{ave}} = \frac{V_{\text{sp}}}{V_{\text{UC}}} \cdot \varrho_{\text{sp}} \tag{2}$$

where ϱ_{sp} is the density of the solid material from which the cells are made. It should be noted that the volume of the unit cell (UC) can be expressed as the sum of solid and free volume as:

$$V_{\text{UC}} = V_{\text{so}} + V_{\text{free}} \tag{3}$$

A further important field is the comparison between the experimental tests with a rather random arrangement of spheres and the simulation results with the idealised arrangement of spheres. Real hollow sphere structures show a rather random arrangement of the spheres. On the other hand, many modelling (i.e. this paper) approaches are based on periodic geometries and structures which possess different packing densities such as primitive cubic (pc), body-centered cubic (bcc), face-centered cubic (fcc) and hexagonal closest (hc) (cf. Fig. 5). Knowing the packing density of the real structure, one may assign the proper topology for modelling the structure or use the result to interpolate model calculations based on the simplified periodic structures [24]. The results are plotted over the average density to be comparable with the experimental results which are currently under development.

7 Results

Figure 10 shows the normalised conductivity over the average density for sintered hollow sphere structures. It can be seen that the heat conductivity is increasing when the average density is increasing (the hole diameter is decreasing). In addition, one can observe that the results for different types of arrangements including primitive cubic (PC), face centred cubic(FCC), body centred cubic (BCC) and hexagonal (HEX) have a linear behaviour depending on the average density. That means that the thermal conductivity is much more influenced by the average density than by different types of arrangements.

Also the influence of the hollow spheres' wall thickness on the thermal conductivity has been studied for sintered PHSS. Decreasing the wall thickness reduces the thermal conductivity, e.g. when the wall thickness decreases from 0.1 mm to 0.07 mm, the thermal conductivity is also decreased. Table 2 summarises this reduction for different configuration.

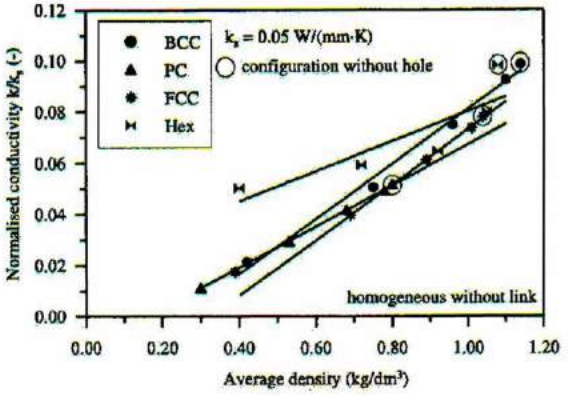

Figure 10: Normalised effective thermal conductivity as a function of relative density for different hole arrangements in the case of sintered spheres.

Hole diameter	FCC	PC	BCC	HEX
$0d_s$	31.96%	31.67%	31.8%	28.74%
$0.25d_s$	31.93%	31.76%	35.13%	37.50%
$0.5d_s$	31.86%	32.12%	33.16%	38.10%
$0.75d_s$	40.66%	32.38%	40.64%	32.49%
$1d_s$	29.55%	33.10%	53.16%	40.36%

Table 2: Reduction of thermal conductivity when the wall thickness of the hollow sphere is reduced from 0.1 mm to 0.07 mm for different hole diameters (1d is the case where the largest possible hole is located between the sintering areas with $d_s = 1.47$ mm, cf. Fig. 8)

8 Outlook

In the scope of this research project, the effective thermal conductivity of perforated hollow sphere structures has been numerically estimated and compared to configurations without holes for the case that hollow spheres are sintered together. Introducing holes in the sphere shells clearly reduces the thermal conductivity of the HSS. Also reducing of the wall thickness in hollow spheres reduce the thermal conductivity. In addition, it is true to say that the thermal conductivity is much more influenced by the average density than by different types of arrangements. The numerical approach has been based on unit cells study. Future investigations must clarify the influence of the hole arrangement and geometrical modifications.

References

[1] Lu, W., Zhao, C.Y., Tassou, S.A., "Thermal Analysis on Metal-Foam Filled Heat Exchangers. Part I: Metal-Foam Filled Pipes," *Int J Heat Mass Tran*, V49, N15-16, pp. 2751-2761, 7/06.

[2] Lu, T.J., Stone, H.A., Ashby, M.F., "Heat Transfer in Open-Cell Metal Foams,", *Acta Mater*, V46, N10, pp. 3619-3635, 6/98.

[3] Boomsma, K., Poulikakos, D., Zwick, F.,"Metal Foams as Compact High Performance Heat Exchangers,", *Mech Mater*, V35, N12, pp. 1161-1176, 12/03.

[4] Lu, T.J., Chen, C., "Thermal Transport and Fire Retardance Properties of Cellular Aluminium Alloys," *Acta Mater*, V47, N5, pp. 1469-1485, 3/99.

[5] Schneider, L., Boehm, A., Korhammer, C., Scholl, R., Voigtsberger, B., Stephani, G., US Patent 6501784. (2002).

[6] Baumeister, E., Klaeger, S., Kaldos, A., "Lightweight, Hollow-Sphere-Composite (HSC) Materials for Mechanical Engineering Applications," *J Mater Process Tech*, V155, Special Issue: Part 2 Sp. Iss. SI, pp. 1839-1846, 11/04.

[7] Lu, K.T., Kou, H.S., "Combined Boundray avd Inertia Effects for Fully-Developed Mixed Convection in a Vertical Chanel Enbeded in Porous-Media," *Int Commun Heat Mass*, V20, N3, pp. 333-345, 6/93.

[8] Fiedler, T., Öchsner, A., "On the Thermal Conductivity of Adhesively Bonded and Sintered Hollow Sphere Structures (HSS)," *Mat Sci Forum* V553, pp. 39-44, 8/07.

[9] Fiedler, T., Öchsner, A.,"Influence of the Morphology of Joining on the Heat Transfer Properties of Periodic Metal Hollow Sphere," *Mat Sci Forum* V553, pp. 39-44, 8/07.

[10] Fiedler, T., Solórzano, E., Öchsner, A., "Numerical and Experimental Analysis of the Thermal Conductivity of Metallic Hollow Sphere Structures," *Mater Lett*, V62, N8-9, pp. 1204-1207, 3/08.

[11] Fiedler, T., Öchsner, A., Belova, I.V., Murch, G.E., "Recent Advances in the Prediction of the Thermal Properties of Syntactic Metallic Hollow Sphere Structures," *Adv Eng Mater*, V10, N4, pp. 361-365, 4/08.

[12] Glatt GmbH, Binzen, Germany, private communication (2007).

[13] Jäckel, M., German Patent, 1987,724 (3),156.

[14] Jäckel, M., German Patent, 1983, 210(3),770.

[15] Studnitzky, T., Andersen, O., *Cellular Metals and Polymers*, Trans Tech Publications, 2005.

[16] Rousset A., Bonino, J.P., Blottiere, Y., Rossignol, C., French Patent, 1987, 707(8),440.

[17] Degischer, H.P., Kriszt, B., editors, *Handbook of Cellular Metals*, WILEY-VCH,2002.

[18] Veyhl, C., Winkler, R., Merkel, M., öchsner, A., "Structural Characterisation of Diffusion-Bonded Hollow Sphere Structure," *Defect and Diffusion Forum*, V280-281, pp. 85-96, 11/08.

[19] de Graef, M., McHenry, M., *Structure of Materials, An Introduction to Crystallography, Diffraction and Symmetry*, Cambridge: Cambridge University Press; 1997.

[20] Benzley, S.E., Perry, E., Merkle, K., Clark, B., Sjaardema, G.F., "A comparison of allhexagonal and alltetrahedral finite element meshes for elastic and elastic-plastic analysis," Fourth International Meshing Roundtable, , Albuquerque, New Mexico, pp. 179b 191, 10/95.

[21] Fiedler, T., Sturm, B., Öchsner, A., Gracio, J., Kuhn, G., "Modelling the mechanical behaviour of adhesively bonded and sintered hollow sphere structures," *Mech Compos Mater*, V42, N6, pp. 559-570, 11/06.

[22] Fiedler, T., PhD Thesis, University of Aveiro, Portugal, 2007.

[23] Gibson, L.J., Ashby, M.F., *Cellular solids: structures & properties*, Cambridge University Press, Cambridge, 1997.

[24] Veyhl, C., Master Thesis, University of Applied Science Aallen, Germany, 2008.